Ceramics International 43 (2017) 7663–7667

Contents lists available at ScienceDirect

Ceramics International

journal homepage: www.elsevier.com/locate/ceramint

BSCCO superconductor micro/nanofibers produced by solution blow-spinning technique

C.R. Cena[a,*], G.B. Torsoni[b], L. Zadorosny[c], L.F. Malmonge[c], C.L. Carvalho[c], J.A. Malmonge[c]

[a] UFMS – Federal University of Mato Grosso do Sul, Campo Grande-MS, Brazil
[b] UEMS – State University of Mato Grosso do Sul, Dourados-MS, Brazil
[c] Universidade Estadual Paulista (UNESP), Faculdade de Engenharia, Campus de Ilha Solteira, Avenida Brasil, 56, Centro, 15385-000 Ilha Solteira-SP, Brazil

ARTICLE INFO

Keywords:
Solution blow-spinning
Nanofibers
Superconductor
Bi-2212

ABSTRACT

This paper presents the synthesis and characterization of BSCCO superconducting fibers synthesized by heat-treating poly(vinyl pyrrolidone) (PVP)/BSCCO precursor microfibers produced by the solution blow-spinning technique. Different concentrations (v/v) of the BSCCO precursor were added to the PVP solution to evaluate the influence of solution viscosity on fiber morphology. The production of PVP/BSCCO microfibers and their morphology were strongly influenced by the volatility of the solvent and the concentration of the added BSCCO in the solution. After heat-treatment, fibrous structures were obtained for the BSCCO system. The structural properties of the samples were analyzed by scanning electron microscopy (SEM) and X-ray diffraction (XRD). The XRD pattern revealed the formation of $Bi_2Sr_2Ca_1Cu_2O_x$ and $Bi_{1,9}Sr_{1,8}CuO_{5,5}$ phases. Finally, electrical measurements (R×T) showed electrical resistance decay at the transition temperature (Tc) that was typical of that observed in superconductor materials.

1. Introduction

In the last few decades, many studies have focused on the processing of nanomaterials [1–3]. This is because this is a relatively new research area; furthermore, nanomaterials show new properties and promise new applications owing to their different morphology and scale [4,5].

Many techniques have been developed in the search for different nanomaterial morphologies [5–11]. For example, Medeiros et al. [12] reported the solution blow-spinning (SBS) technique as an alternative to the well-established electrospinning technique [13] for the production of polymeric fibers. SBS affords advantages such as higher rate of fiber production, low production cost, and easy implementation. SBS basically involves the use of two concentric needles, where air or another gas is ejected at high pressure through the external channel and a polymer solution is simultaneously ejected through the internal channel. The polymer solution is injected at a constant rate by a needle in the internal channel. One drop of solution is formed at the needle tip. By the action of drag forces originating from the pressure difference caused by the air flow, this drop is stretched to form a fiber jet. The jet is ejected from the needle tip, and it then accelerates to form polymer fibers [12,14].

The synthesis of nanomaterials with different geometries, such as fibers, has become easier over the years, and it may lead to the development of novel materials with new properties and/or technological applications. Nanostructured ceramic fibers have attracted much research interest because they show great potential for applications and phenomenological studies owing to their geometry [5–7]. High-temperature superconducting materials like $Bi_2Sr_2Ca_{n-1}Cu_nO_{2\ n+4+x}$ (BSCCO) and $YBa_2Cu_3O_{7-\delta}$ (YBaCu) are usually produced in different forms, such as thin films, thick films, tapes, wires, and fibers, by traditional methods like spin coating and *powder in a tube*; these materials show great potential for electronic and energy transmission technologies [10,11]. These materials could also be texturized, thereby increasing the superficial area between nearby grains; this improves electrical junctions and aligns superconductor planes [15–21]. Recently, BSCCO fibers were obtained by the electrospinning technique [10] by using a sol-gel precursor; these fibers had an average diameter of 150–250 nm with Tc of ~78.7 K. Furthermore, our research group has synthesized YBaCu fibers by SBS [22].

In this paper, we present a potential route for synthesizing BSCCO superconductor fibers by SBS [23]. The SBS technique was used to produce composite microfibers of poly(vinyl pyrrolidone) (PVP)/BSCCO. These were heat-treated to produce BSCCO superconductor

* Corresponding author.
E-mail address: cicero.cena@ufms.br (C.R. Cena).

http://dx.doi.org/10.1016/j.ceramint.2017.03.065
Received 21 February 2017; Received in revised form 9 March 2017; Accepted 10 March 2017
Available online 14 March 2017

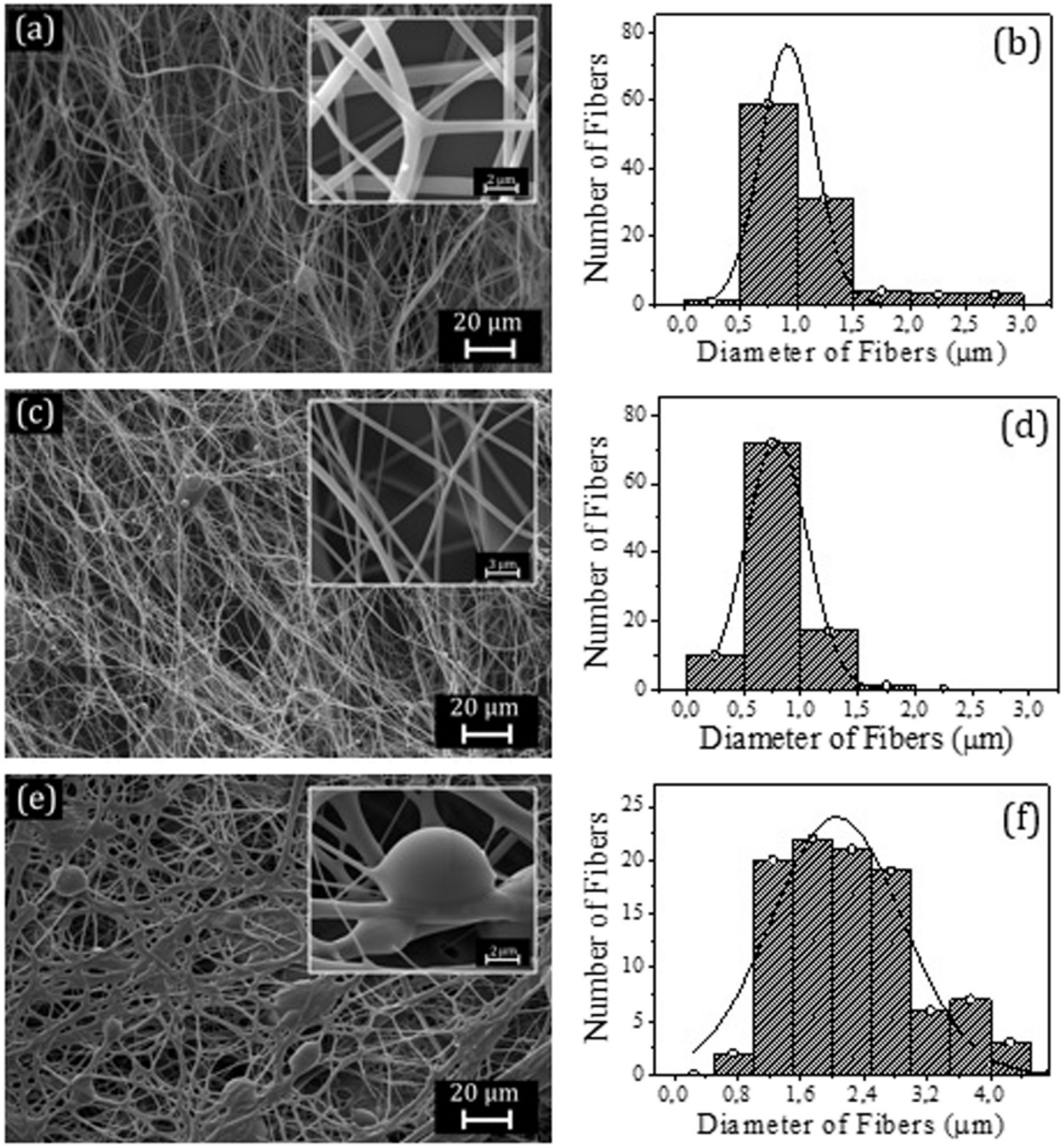

Fig. 1. PVP/BSCCO composite fibers, SEM images, and diameter distribution analysis: (a–b) 10 vol%, (c–d) 15 vol%, and (e–f) 20 vol% of BSCCO added to PVP. Fiber details Inset. Before heat-treatment.

nanofibers. The morphological, structural, and electrical properties of the obtained nanofibers were investigated.

2. Materials and methods

2.1. Precursor solution preparation

PVP, (C6H9NO)n, with average molecular weight of 360.000 was supplied in powder form by Sigma-Aldrich Chemical Company. The PVP solvent was a mixture of isopropyl alcohol (AI) (C_3H_8O) and deionized water in 90:10 (v/v) proportion. The polymer concentration was kept at 0.10 g/mL.

The superconductor ceramic precursor solution was synthesized using a stoichiometric composition of $Bi_2Sr_2Ca_1Cu_2O_x$ (BSCCO-2212). The synthesis route used mixed acetate solutions, as reported previously [24]. Initially, the chemical reagents were dissolved separately in aqueous solution: (1) bismuth nitrate ($Bi(NO_3)_3{\cdot}5H_2O$), by adding ammonium hydroxide (NH_4OH) and glacial acetic acid (CH_3COOH); (2) strontium nitrate ($Sr(NO_3)_2$), by adding ammonium hydroxide (NH_4OH); (3) calcium acetate ($C_4H_6CaO_4$), by adding ammonium hydroxide (NH_4OH) and glacial acetic acid (CH_3COOH); and, finally, (4) copper acetate (II) ($((CH_3COO)_2Cu{\cdot}H_2O$), by adding ammonium hydroxide (NH_4OH).

Finally, the solutions were mixed in the following sequence: (1) calcium solution was added to the strontium solution, (2) copper solution was added to the solution obtained in the previous step, and (3) the solution obtained in the previous step was added to the bismuth solution. Then, glacial acetic acid was added under constant stirring until a pH of ~5.6 (26 °C) was achieved. Finally, a transparent light-blue solution was obtained.

2.2. Sample preparation by solution blow-spinning technique

PVP/BSCCO composite microfibers were produced by the SBS technique [19,20]. Previously defined proportions (in vol%) of the BSCCO precursor solution were added to the PVP solution to determine

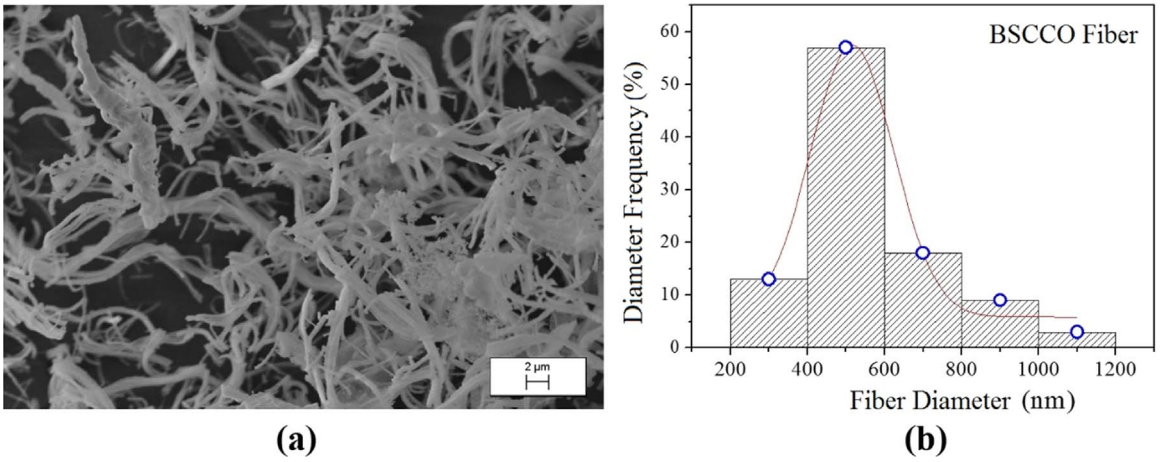

Fig. 2. SEM images (a) and fiber diameter distribution (b) of ceramic fibers obtained from PVP-10%BSCCO (BSCCO10%) and heat-treated at 850 °C/2 h at a heating rate of 1 °C/min.

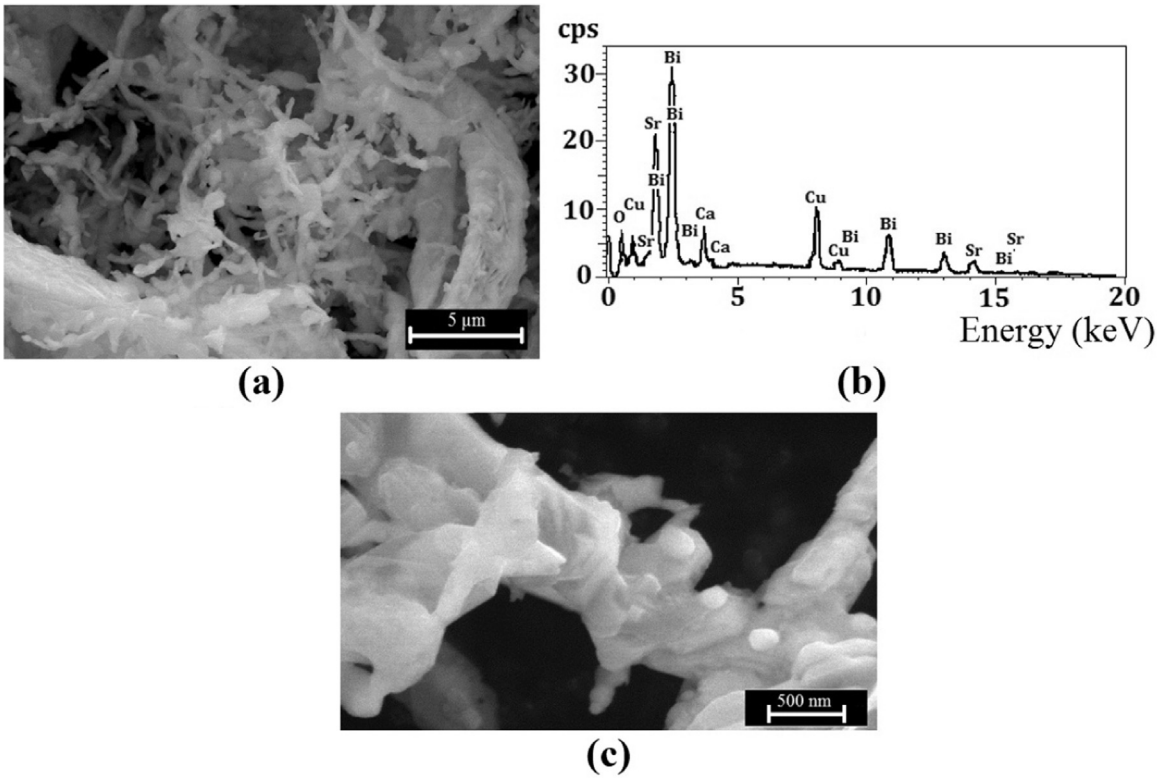

Fig. 3. (a) SEM-FEG images of BSCCO10% ceramic fibers analyzed by EDS, (a) EDS spectrum, and (c) microstructure detail of a nanofiber.

the optimal conditions under which to produce the fibers by SBS. Three conditions were studied: (1) 10 vol%, (2) 15 vol%, and (3) 20 vol%. The SBS standard processing conditions were as follows: injection rate of 0.11 mL/min, gas pressure of 120 kPa, work distance of 25 cm, 5-mm needle protrusion beyond the nozzle base, and needle diameter of ~0.424 mm (around 22 gauge). Finally, the PVP/BSCCO composite microfibers were heat-treated in a conventional furnace at 850 °C for 2 h at a heating rate of 1 °C/min.

2.3. Sample characterization

The fiber morphology was investigated by scanning electron microscopy (SEM; EVO-LS15, ZEISS) and by scanning electron microscopy with a field-emission gun (FEG-SEM; XL 30, Philips). The fiber diameter distribution and average diameter were measured using IMAGE J (National Institutes of Health, USA) software analysis by examining 100 random fibers from SEM images with 1000x magnification. The microstructural properties of the samples were determined by X-ray diffraction (XRD; XRD-600, Shimadzu) with CuKα (1.54060 Å) radiation and operating at 30 kV and 40 mA. The crystalline phases were identified by using X-ray patterns from the Inorganic Crystal Structure Database (ICSD). Then, the crystallite size was estimated by using the Scherrer equation [25] according to literature [26], by considering a typical value of 0.94 for the shape factor.

Finally, the superconductor's characteristic behavior (critical temperature transition) was evaluated through electrical measurements. The obtained fibers/powders were pressed into cylindrical pellets, and their electrical resistance was measured as a function of the sample temperature (R×T). Electrical measurements were performed using the DC four-probe method; a transport current of 5 mA was applied using a current/voltage source (228 A, Keithley Instruments). Cooling was performed by immersing the sample holder in liquid nitrogen.

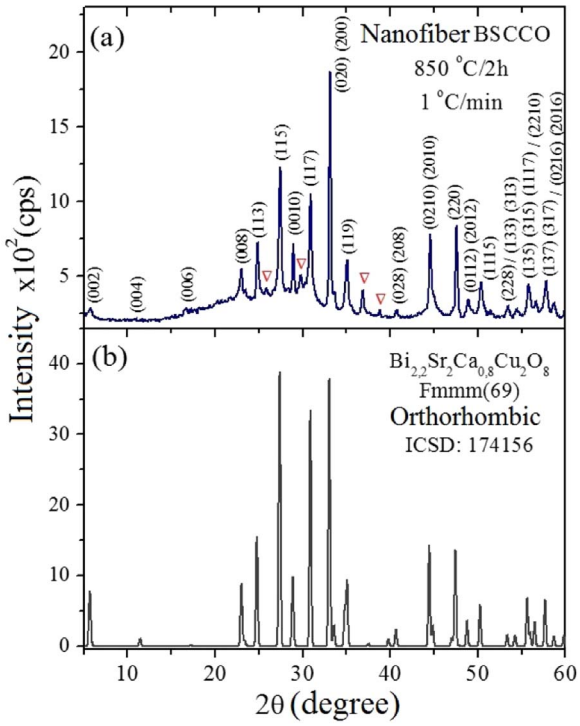

Fig. 4. XRD pattern for (a) BSCCO10% fiber and (b) XRD pattern obtained from ICSD. The crystallographic phases were identified as $Bi_{2,2}Sr_2Ca_{0,8}Cu_2O_8$ (Bi-2212) (ICSD: 174153), indicated in the figure by the Miller indices (*hkl*), and $Bi_{1,9}Sr_{1,8}CuO_{5,5}$ (Bi-2201) (ICSD: 71910), indicated in the figure by the inverted Δ symbol.

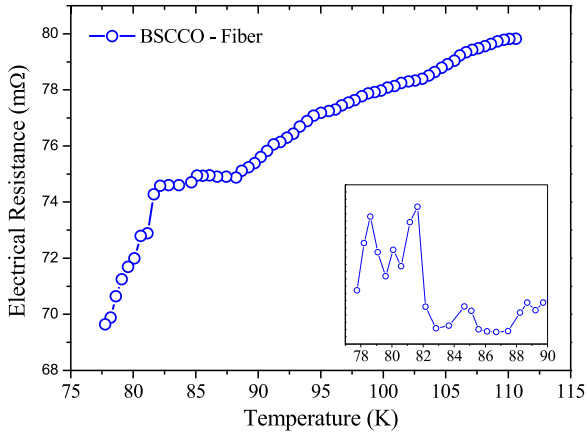

Fig. 5. Electrical resistance vs temperature for BSCCO10% ceramic. The inset shows the derivative of the resistance plotted as a function of temperature.

3. Results and discussion

PVP/BSCCO microfibers were successfully produced by mixing 10, 15, and 20 vol% BSCCO precursor solution with the PVP solution, as shown at Fig. 1. The typical fiber morphology formed was shown to be related to the concentration of the BSCCO solution added to the PVP solution. Microfibers produced with a 10 vol% BSCCO precursor solution (Fig. 1(a)) showed a predominantly smooth and homogeneous morphology; only a few defects, such as entire drops and beads, could also be identified [27]. The fiber diameter distribution histogram (Fig. 1(b)) showed a narrow and well-defined shape, with a maximum value centered at ~980 nm.

Fig. 1(c) shows similar PVP/BSCCO fiber formation behavior for 15 vol% of BSCCO added to PVP solution. Although the fiber diameter distribution histogram (Fig. 1(d)) showed a maximum centered at ~800 nm, the fiber thickness was ~100 nm smaller, compared to those produced with 10 vol% of BSCCO. The decrease in fiber diameter can be associated with lower viscosity of the solution owing to the addition of more solvent to the BSCCO solution. Adding more solvent facilitated fiber stretching during the processing, resulting in lower fiber diameter. Upon adding 20 vol% BSCCO to PVP (Fig. 1(e)), the microfibers produced showed much fusion and coalescence between the contact points, and consequently, there was a large increase in morphological defects such as beads and ramifications. This behavior is typical for systems with low concentration (high amount of solvent), where lower solvent evaporation makes fiber formation difficult [28,29].

Ceramic nanofibers (or submicrometer fibers) were successfully produced after heat-treating PVP/BSCCO precursor microfibers with 10 vol% of BSCCO at 850 °C for 2 h, as shown in Fig. 2. This sample was called BSCCO10%. Microfibers with 10 vol% of BSCCO were chosen as the ceramic precursor because they showed better morphology and aspect ratio compared to the green fiber before heat-treatment).

Fig. 2(a) shows the heat-treated ceramic nanofibers; despite their relatively short length, continuous fibers can be identified. The short length can be attributed to the low amount of inorganic materials in the precursor green fibers, which should react during heat-treatment to form the ceramic fiber. The fiber diameter distribution histogram (Fig. 2(b)) was narrow with a maximum centered at ~500 nm. The average fiber diameter was estimated to be ~568 nm.

Energy dispersive spectroscopy (EDS) was used to qualitatively study the fiber chemical composition. Fig. 3(a) shows the analyzed region of the sample; a typical fibrous morphology could be seen. The EDS spectra (Fig. 3(b)) indicate that the fibers have the expected chemical composition, with the relative intensity between the peaks being in accordance with stoichiometric $Bi_2Sr_2Ca_1Cu_2O_x$. Fig. 3(c) shows a fibrous structure with plate-like grains that is characteristic of the Bi-2212 [30] superconductor material; it forms a continuous length with ~500-nm diameter in accordance with the histogram shown in Fig. 2(b). The higher-magnification image (Fig. 3(d)) shows some regions with granular morphology that are probably associated with the secondary phase Bi-2201.

The phase formation of the fibrous ceramic BSCCO10% was investigated by XRD diffraction (Fig. 4). The diffraction pattern was compared with those reported in literature [31,32] from the ICSD by using a monocrystal XRD pattern with the composition $Bi_{2,2}Sr_2Ca_{0,8}Cu_2O_8$ (Bi-2212) and orthorhombic structure.

The analyzed sample was characterized as a polyphasic material; its main phase was identified as $Bi_{2,2}Sr_2Ca_{0,8}Cu_2O_8$ (Bi-2212) [31] with orthorhombic structure, indicated by the Miller index (*hkl*) in Fig. 4(a). The secondary phase was identified as $Bi_{1,9}Sr_{1,8}CuO_{5,5}$ (Bi-2201) [32] with monoclinic structure, indicated by the inverted Δ symbol in Fig. 4(a). The relative intensity between the diffraction peaks differs slightly from the pattern reported in literature (Fig. 4(b)) owing to crystallographic phase deviation. Although Bi-2201 also shows superconductor properties, compared to a pure Bi-2212 superconductor, its phase is undesirable because it influences the superconductor properties of the fibers. Bi-2201 formation can be related to the stoichiometry deviation, preparation route, and/or heat-treatment.

The crystallite size was estimated to be ~160 nm by using the Scherrer equation [26]. This value was larger than those reported in literature, which varied between 20 and 81 nm [30,33] for powders produced by sol-gel synthesis and thin films, respectively. This suggests that fibers produced by SBS, as described before, are probably subjected to some microstructural modifications, maybe owing to the directional growth of the grains, and this reflects in changes in the crystallite size. Another factor that can contribute to a peak broadening (FWHM) (used in the Scherrer equation for grain size calculation) is the intrinsic microstructural strain.

The principal characteristic of a superconductor material is a sharp decline in electrical resistance at the transition from the normal to the superconductor state at the critical temperature (Tc) [34,35]. Fig. 5

shows the electrical resistance versus temperature behavior of the BSCCO10% sample. Ohmic behavior can be observed above 90 K; below this temperature, electrical resistance decreases sharply with temperature, suggesting a potential transition from the normal to the superconductor state of the sample, as discussed in literature [30]. The sample has biphasic nature (Bi-2212 and Bi-2201), and it shows nonzero resistance at 70 K owing to the presence of the Bi-2201 phase, which is in the normal state.

Our nanofiber sample showed normal to superconductor state transition with a smooth and double inflection point. The critical temperature (Tc) was determined by the derivative method; inflections occurred at 78.6 and 81.6 K, and both Tcs were assigned to the BSCCO-2212 superconductor phase [18,30,34]. According to literature [35], a small decrease in Tc value can be related to the weak link between adjacent superconductors grains. The BSCCO-2201 superconductor transition occurs at a lower temperature of ~20 K, and it could not be observed in our study owing to experimental limitations.

4. Conclusion

The SBS technique showed great potential for producing BSCCO superconductor nanofibers. Although PVP/BSCCO composite fibers were obtained successfully, continuous and homogeneous ceramic nanofiber formation was not observed, probably owing to the low amount of ceramic precursor available in the composite fibers during heat-treatment.

XRD analysis showed the coexistence of Bi-2212 and Bi-2201 crystallographic phases in the final ceramic fibers. The crystallite size was estimated to be ~160 nm; this value is much higher than those reported in literature for BSCCO superconductors produced as powder or thin films.

Electrical measurements of the pellets produced from BSCCO nanofibers revealed the typical electrical resistance versus temperature curve (R×T) observed for superconductor materials. The sample analyzed showed two inflection points in the R×T curve at 78.6 and 81.6 K; these were attributed to the Bi-2212 superconductor transition.

Our results point to a promising route to produce BSCCO superconductor nanofibers with great potential for new applications or basic studies by using a low-cost technique.

Acknowledgment

One of the authors (C. S.S) is grateful to the “Coordenação de Aperfeiçoamento de Pessoal de Nível Superior (CAPES)” for the student fellowship.

References

[1] D. Li, Y. Xia, Direct fabrication of composite and ceramic hollow nanofibers by electrospinning, Nano Lett. 4 (2004) 933–938.
[2] R.G.F. Costa, J.E. Oliveira, G.F. Paula, P.H.S. Picciani, E.S. Medeiros, C. Ribeiro, L.H.C. Mattoso, Eletrofiação de polimeros em solução. Parte II: Aplicações e perspectivas, Polímeros: Ciência e Tecnol. 22 (2012) 178–185.
[3] C.R. Cena, A.K. Behera, B. Behera, Structural, dielectric, and electrical propertiesod lithium niobate microfibers, J. Adv. Ceram. 5 (2016) 84–92.
[4] C. Vakifahmetoglu, Fabrication and properties of ceramic 1D nanostructures from preceramic polymers: a review, Adv. Appl. Ceram. 10 (2011) 188–204.
[5] Y. Huang, G.F. Fuente, A. Sotelo, A. Badia, F. Lera, R. Navarro, C. Rillo, R. Ibanez, D. Beltran, F. Sapina, A. Beltran, (Bi, Pb)2Sr2Cu3O10-δ superconductor composites: ceramics vs fibers, Physica C 185 (1991) 2401–2402.
[6] R. Ramaseshan, S. Sundarrajan, R. Jose, S. Ramakrishna, Nanostructures ceramics by electrospinning, J. Appl. Phys. 102 (2007) 1–18.
[7] D. Li, Y. Xia, Electrospinning of nanofibers: reinventing the wheel?, Adv. Mater. 16 (2004) 1151–1170.
[8] Y. Dai, W. Liu, E. Formo, Y. Sun, Y. Xia, Ceramic nanofibers fabricated by electrospinning and their applications in catalysis, environmental science, and energy technology, Polym. Adv. Technol. 22 (2011) 326–338.
[9] D. Li, J.T. Maccann, Y. Xia, M. Marquez, Electrospinning: a simple and versatile technique for producing ceramic nanofibers and nanotubes, J. Am. Ceram. Soc. 89 (2006) 1861–1869.
[10] E.A. Duarte, P.A. Quintero, M.W. Meisel, J.C. Nino, Electrospinning synthesis of superconducting BSCCO nanowires, Physica C 495 (2013) 109–113.
[11] X.M. Cui, W.S. Lyoo, W.K. Son, D.H. Park, J.H. Choy, T.S. Lee, W.H. Park, Fabrication of YBCO superconducting nanofibres by electrospinning, Supercond. Sci. Technol. 19 (2006) 1264–1268.
[12] E.S. Medeiros, G.M. Glenn, A.P. Klamcznyski, W.J. Orts, L.H.C. Mattoso, Solution blow spinning a new method to produce micro- and nanofibers from polymer solutions, J. Appl. Polym. Sci. 113 (2009) 2322–2330.
[13] N. Bhardwaj, S.C. Kundu, Electrospinning: a fascinating fiber fabrication technique, Biotechnol. Adv. 28 (2010) 325–347.
[14] J.E. Oliveira, E.A. Moraes, R.G.F. Costa, Nano and submicrometric fibers of poly(D,L-lactide) obtained by solution blow spinning: process and solution variables, J. Appl. Polym. Sci. 122 (2011) 3396–3405.
[15] C.J. Kim, M.R. Guire, C.J. Allen, A. Sayir, Growth and characterization of BSCCO superconducting fibers, Mater. Res. Bull. 26 (1991) 29–39.
[16] M. Onisih, T. Kohgo, Y. Crogusa, K. Watanabe, M. Kyoto, M. Watanabe, Bi-Pb-Sr-Ca-Cu-O superconducting fibers drawn from melt-quenched, Jpn. J. Appl. Phys. 29 (1990) 64–66.
[17] H. Miao, L.A. Diez, L.A. Angurel, J.I. Pena, G.F. Fuente, Phase formation and microstructure of laser floating zone grown BSCCO fibers: reactivity aspects, Solid State Ion. 101 (1997) 1025–1032.
[18] K. Lebbou, A. Yoshikawa, M. Kikuchi, T. Fukuda, M.T.C. Adad, G. Boulon, Superconductor Bi2212 fiber growth from the melt by micro-pulling down technique, Physica C 336 (2000) 254–260.
[19] F.M. Costa, R.F. Silva, J.M. Vieria, Phase transformation kinetics during thermal annealing of LFZ BSCCO superconducting fibers, Physica C 323 (1999) 23–41.
[20] T. Goto, T. Sugishita, K. Kojima, A new fabrication process of YBCO superconducting filament by solution spinning method under ambient pressure, Physica C 171 (1990) 441–443.
[21] M.F. Carrasco, V.S. Amaral, J.M. Vieira, R.F. Silva, F.M. Costa, Anneling time effect on Bi-2223 phase development in LFZ and EALFZ grown superconducting fibres, Supercond. Sci. Technol. 19 (2006) 15–21.
[22] M. Rotta, L. Zadorosny, C.L. Carvalho, J.A. Malmonge, L.F. Malmonge, R. Zadorosny, YBCO ceramic nanofibers obtained by the new technique of solution blow spinning, Ceram. Int. 42 (2016) 16230–16234.
[23] C.R. Cena, G.S. Larios, M.R.R. Bica, T.A. Canassa, G.Q. Freitas, G.B. Torsoni, Desenvolvimento de um sistema blow-spinning de baixo custo para obtenção de microfibras e nanofibras poliméricas e compósitas, Rev. Bras. Física Tecnológica Apl. 2 (2015) 32–44.
[24] D.I. Santos, C.L. Carvalho, R.R. Silva, M.A. Aegerter, U. Balachandran, R.B. Poeppel, Superconducting films made by spin-coating with acetate solutions, Ceram. Trans. Supercond. 18 (1990) 263–269.
[25] N.S. Goncalves, J.A. Carvalho, Z.M. Lima, J.M. Sasaki, Size–strain study of NiO nanoparticles by X-ray powder diffraction line broadening, Mater. Lett. 72 (2012) 36–38.
[26] B.E. Warren, X-ray Diffraction, Dover Publication, New York, 1990.
[27] H. Fong, I. Chun, D.H. Reneker, Beaded nanofibers formed during electrospinning, Polymer 40 (1999) 4585–4592.
[28] Q. Yang, Z. Li, Y. Hong, Y. Zhao, S. Qiu, C.E. Wang, Y. Wei, Influence of solvents on the formation of ultrathin uniform poly(vinyl pyrrolidone) nanofibers with electrospinning, J. Polym. Sci. 42 (2004) 3721–3726.
[29] L. Wannatong, A. Sirivat, P. Supaphol, Effects of solvents on electrospun polymeric fibers: preliminary study on polystyrene, Polym. Int. 53 (2004) 1851–1859.
[30] J.B. Silveira, C.L. Carvalho, G.B. Torsoni, H.A. Aquino, R. Zadorosny, Thermal treatment of superconductor thin film of the BSCCO system using domestic microwave oven, Physica C 478 (2012) 56–59.
[31] S.A. Sunshine, T. Siegrist, L.F. Schneemeyer, D.W. Murphy, R.J. Cava, B. Batlogg, R.B. Dover, J.V. Fleming, S.H. Glarum, S. Nakahara, R. Farrow, J.J. Krajewski, S.M. Zahurak, J.V. Waszczak, J.H. Marshall, P. Marsh, L.W. Rupp, W.F. Peck, Structure and physical properties of single crystals of the 84-K superconductor Bi2.2Sr2Ca0.8Cu2O8+δ, Phys. Rev. B 38 (1988) 893–896.
[32] H. Leiligny, S. Durcok, P.H. Labbe, M. Ledesert, B. Ravean, Acta Crystallogr. 48 (1992) 407–418.
[33] Y. Zhang, H. Yang, M. Li, B. Sun, Y. Qi, Cryst. Eng. Comm. 12 (2010) 3046–3051.
[34] K. Togano, H. Kamakura, H. Maeda, K. Takahashi, M. Nakao, Preparation of high Tc Bi-Sr-Ca-Cu-O superconductors, Jpn. J. Appl. Phys. 27 (1988) 323–324.
[35] J.R. Schrieffer, Handbook of high temperature superconductivity theory and experiment. New York, Great Britain, 2007.